Anticipating QLCS Tornadogenesis: The Three-Ingredient Method during the 19-20 February 2017 South-Central Texas Tornadic QLCS Event

Brett M. Williams*, Jared Allen and Jon W. Zeitler
NOAA National Weather Service
WFO Austin/San Antonio

Introduction

Quasi-linear convective systems (QLCS) are organized lines of convection that commonly occur over portions of the United States. While the majority of severe weather associated with QLCS comes in the form of strong straight-line winds and marginally severe hail, tornadoes can also be produced by QLCSs (Smith et al. 2012). Research from Trapp et al. (2005) showed that out of 3828 tornadoes occurring in a three year period, about 18% of them were produced by a QLCS. While the majority of tornadoes produced from QLCSs are weak, on the EF-0 to EF-1 scale, a few can reach EF-2 and EF-3 rating, posing a serious threat to life and property.

QLCSs present a unique challenge for a warning forecaster at a National Weather Service (NWS) weather forecast office (WFO). The system can change rapidly, evolving from relatively benign to producing numerous mesovortices within a short period of time. Furthermore, mesovortices, the parent circulation from which QLCS tornadoes are spawned, typically exist within the lowest few kilometers of the surface and can quickly develop and intensify (Houze 2004). This can make it very difficult to identify mesovortices on radar, especially if the QLCS of interest is at a great distance from a WSR-88D radar, in which the rotation may be below the lowest elevation angle. Furthermore, there is the threat for tornadoes to theoretically form in many locations along the QLCS convective line, as opposed to only one area favored for tornadogenesis within a supercell (Newman and Heinselman 2012). Tessendorf and Trapp (2000) note that issuing appropriate severe weather warnings for QLCS tornadoes is problematic, as there are oftentimes no readily identifiable radar precursors preceding such tornadoes with substantial lead time. Due to all of these factors, NWS performance on QLCSs is significantly worse compared to supercells. Brotzge et al (2013) showed that probability of detection (POD) and lead time are significantly poorer for QLCSs compared to supercells. The POD and lead time for QLCS tornadoes was only 50% and twelve minutes compared to 90% and seventeen minutes for a right-moving discrete supercell (Figure 1). This also makes it quite difficult to keep NWS core partners, such as media and local emergency managers, abreast of the immediate and short-term threat areas for tornadoes during QLCS events. It is evident that NWS performance on QLCS tornadoes could stand to be improved to further the NWS mission of protecting life and property.

This study will present a methodology that has been developed with the goal to improve performance during QLCS events by better anticipating the formation and intensification of mesovortices, known as the Three-Ingredient Method. This study will then apply this method to a prolific tornadic QLCS that

* Corresponding author address: Brett M. Williams, NOAA/NWS Austin/San Antonio WFO, 2090 Airport Road, New Braunfels, TX 78130. Email: brett.williams@noaa.gov

occurred in the late evening hours of 19 February 2017 and into the early morning hours of 20 February 2017 across the San Antonio and Austin metro areas in south-central Texas. Lastly, some suggestions for best practices for operational use of this method will be presented.

Background

a. The Three-Ingredient Method

The Three-Ingredient Method for anticipating QLCS mesovortexgenesis was developed by Schaumann and Przybylinkski (2012) in an effort to improve performance in QLCS events. Their study analyzed numerous progressive mesoscale convective system (MCS) cases across many regions of the United States and found three co-existing ingredients which seemed to support an increased likelihood for QLCS mesovortexgenesis. Each of the three ingredients will be discussed and explained in their own respective paragraph below.

The first ingredient is to identify regions of a QLCS line in which the system cold pool and ambient low-level wind shear are nearly balanced or slightly shear dominant along the updraft/downdraft convergence zone (UDCZ). This balance creates a deeper, more upright updraft which leads to more efficient vertical tilting and stretching of horizontal vorticity along the UDCZ (Figure 2). The balance of the cold pool and wind shear can be gauged in real-time by how well the leading edge in the QLCS reflectivity line correlates to the UDCZ, which is essentially the gust front of the QLCS. If the UDCZ is perfectly co-located with the leading edge in reflectivity, then the QLCS at that point can be assessed as being balanced. If the UDCZ is displaced out ahead of the leading edge in reflectivity, then the QLCS is cold pool dominant. If the leading edge in reflectivity is displaced out ahead of the UDCZ, then the QLCS is wind shear dominant.

The second ingredient is to identify regions of a QLCS line in which the 0-3 km line-normal bulk shear magnitudes are equal to or greater than 30 knots. Increasing values of line normal wind shear correlates to increasing likelihood of mesovortexgenesis. Line normal wind shear is calculated by finding the angle between the QLCS storm motion vector and the 0-3 km shear vector and applying the cosine function. An example of this calculation can be found in Figure 3. The line-normal shear magnitudes can evolve quickly if the motion of the QLCS is changing, and can vary across different specific regions of the QLCS. Line-normal wind shear increases as the wind shear vector becomes more perpendicular to the QLCS orientation and parallel to the QLCS motion. The 0-3 km line normal wind shear can be viewed in AWIPS by a warning forecaster by using the volume browser and selecting the RAP model 0-3 km wind shear. Another method for analyzing the 0-3 km bulk shear is viewing it from the Storm Prediction Center (SPC) mesoanalysis page.

The third ingredient is to look for surges or bows in the QLCS line due to rear inflow jets (RIJ) or local outflow enhancements. Evidence of a RIJ include a rear-inflow notch, a bowing feature in reflectivity, or an outflow surge in velocity. This component has multiple possible effects on the QLCS. First, surges or bowing segments can affect the line-normal 0-3 km shear magnitudes. If the 0-3 km shear vector is out of the southwest at around 220° and a QLCS line is moving from the west (270°), an outflow surge causing a change in the QLCS motion to more out of the southwest (closer to 220°) acts to increase the 0-3 km line normal bulk shear magnitude. Additionally, an enhanced updraft is created along the leading edge in the convective outflow/gust front surge in the bowing segment, which acts to further stretch the vertical vorticity and increase low-level rotation.

b. Mesovortex Formation and the Three-Ingredient Method

To help make sense of the how the Three-Ingredient Method physically relates to mesovortexgenesis, it is important to understand the processes behind mesovortices. Funk et al. (1999) found that mesovortexgenesis usually occurs as a low-level cyclonic convergent area along the leading edge of the bow apex and that tornadoes tended to occur during the intensification and deepening of this low-level vortex. Weisman and Trapp (2003 Part I) found that the magnitude of the wind shear, especially at low-levels, had large implications on mesovortexgenesis. For weaker shear cases (less than 15 ms^{-1} over the lowest 2.5 km), weak cyclonic vortices developed along leading edge of gust front, but they remained very shallow (less than one km) and were not associated with the mid-level updraft. As shear increased in both magnitude and depth, bowing segments became more prevalent, with stronger low-level vortices located beneath a midlevel updraft leading to deeper vertical stretching. Atkins and St. Laurent (2009 Parts I & II) presented a two-part study that examined the genesis of low-level mesovortices formed within bow echoes. Part I found that stronger and more numerous mesovortices were formed when the low level environmental shear nearly balanced the horizontal shear produced by the cold pool, creating upright updrafts. The difference between a QLCS with a balance between the low-level wind shear and the cold pool resulting in upright updrafts and strong mesovortices and a QLCS with weak low-level shear and a dominating cold pool resulting in significant upshear tilting and weak or completely absent mesovortices can be found in Figure 4. Note how the RIJ descends steeply immediately behind the leading convective line in the severe QLCS compared to the gradual descent of the RIJ well behind the leading convective line in the non-severe QLCS. Also, note the much more organized appearance in reflectivity associated with the severe QLCS, with the leading convective line right up against the gust front and the presence of a rear-inflow notch and accompanying appendage on the leading edge of the convective line. Mesovortices are common in this location due to the presence of an updraft above the mesovortex formation region. Furthermore, they found that as the magnitude of the deep-layer shear increased, both the strength and the number of mesovortices increased accordingly. Atkins and St. Laurent (2009 Part II) found that a local updraft maximum, which was created by a strong downdraft that produced a bulging in the gust front, tilted baroclinically generated vortex lines upward into arches, ultimately forming the vortex couplet of the mesovortex (Figure 5). As the QLCS evolved into the mature bow echo stage, mesovortices of the cyclonic-only variety were primarily observed, which formed from the tilting of baroclinic horizontal vorticity by the downdraft in association with the RIJ. Schenkman et al. (2012) also suggested that an outflow surge and a strong low-level updraft is critical in converging and amplifying vertical vorticity associated with the mesovortex (Figure 6).

Ultimately, while these studies suggested a few different specific mechanisms for mesovortex formation, they all found that the key to mesovortex formation lies in the updraft and downdraft processes within the QLCS as well as the presence of strong low-level wind shear. These studies converged on the following main processes for how mesovortices are generated. First, that mesovortexgenesis is initiated at low levels by tilting of crosswise baroclinic horizontal vorticity by the downdraft (Trapp and Weisman 2003 Part II, Wheatley and Trapp 2008, Atkins and St. Laurent 2009). Second, that a strong low-level updraft is essential to stretch the vertical vorticity associated with the mesovortex (Schenkman et al. 2012, Atkins and St. Laurent 2009). Lastly, that strong low-level wind shear is critical to the formation and strengthening of mesovortices, and that the stronger the wind shear, the more probable that the vorticity within the low-level mesovortex can be further stretched by a mid-level updraft (Trapp and Weisman 2003 Part I, Atkins and St. Laurent 2009 Part I).

This research gives validation to the merits of the Three-Ingredient Method, suggesting that the method has physical connections to the formation of mesovortices rather than being just a coincidental correlation.

Event Summary and Application of the Three-Ingredient Method

a. General Event Overview

A tornadic QLCS impacted the Austin/San Antonio NWS (EWX) County Warning Area (CWA) on the late evening hours of Sunday, 19 February 2017 and continuing into the early morning hours of Monday, 20 February 2017. This QLCS produced a total of 9 confirmed tornadoes across the San Antonio and Austin metro areas (Figure 7). Three of these 9 tornadoes were rated EF-2, with one of these EF-2 tornadoes causing significant, widespread damage to a densely populated neighborhood of north-central San Antonio and the city of Alamo Heights. This was the largest tornado event in the month of February for the EWX CWA, and was the second largest tornado event in over a decade in terms of number of tornadoes.

b. Pre-Storm Environment

While the purpose of this paper is primarily to apply the Three-Ingredient Method to this particular event, a general overview of the synoptic set up and pre-storm environment will be presented for context.

At 00z on 20 February 2017 (6 pm CST 19 February 2017), SPC upper air analysis showed a high-amplitude trough across the southwestern United States and northern Mexico (Figure 8). Strong 300 hPa south/southwesterly winds up to 90 knots were in place across south-central Texas. A 100+ knot jet streak extended from northern Mexico northward into the front range of the Rockies, putting south-central Texas roughly in the right entrance region of the jet streak. The SPC analysis depicted large values of upper level divergence across south-central Texas, with the bulls-eye over the San Antonio region.

At 500 hPa, the high-amplitude trough was observed once more across the southwestern US and northern Mexico (Figure 9). The trough was moving northeastward toward south-central Texas, yielding height falls and positive vorticity advection, creating widespread forcing for ascent across the region. Additionally, 50-60 knot south/southwesterly flow was in place across the region, creating substantial deep layer shear.

The 850 hPa analysis showed ample boundary layer moisture in place across south-central Texas, with 850 hPa dew points on the order of 8 to 10 °C (Figure 10). Winds were out of the south at 25-35 knots, providing a moderately strong low-level jet and continuing to advect moisture from the Gulf of Mexico.

At the surface, a surface low was located across the Texas and Oklahoma panhandles with a pacific cold front draped north to south across west central Texas, moving due east toward the San Antonio and Austin metro areas (Figure 11). The 00z ASOS observation at San Antonio International Airport showed a temperatures of 76 °F, and dew point of 65 °F, with winds out of the southeast at 11 knots. A 00z NAM sounding at the San Antonio airport showed very low LCLs (below 750 meters), ample boundary layer moisture, and sufficient instability of about 1500 J kg^{-1} of surface-based CAPE.

In the hours leading up to the event, the Austin/San Antonio WFO published a graphic to their webpage and social media platforms, as well as sent a partner email to alert the public and core partners of the threat of severe thunderstorms that evening (Figure 12). The primary focus was on the threat for severe winds, with only a very nominal threat for tornadoes. Accordingly, the SPC Day 1 Convective Outlook had a 15% hail and wind probability for south-central Texas, but only a 2% tornado probability. A significant tornado event was not anticipated by the local WFO nor the SPC.

c. Non-tornadic Period of the QLCS and the Three-Ingredient Method

The event began around 00z 20 February 2017 (6 pm CST on 19 February) as semi-discrete cells across northern Mexico and the western counties of the EWX CWA near Del Rio and Rocksprings. By 02z (8 pm CST), the semi-discrete cells had grown upscale and congealed into a MCS/QLCS. The first time period that the Three-Ingredient Method will be applied will be around 230z (or 830 pm CST) west of the San Antonio metro area.

For the first ingredient, a small region of the QLCS in which the cold pool and wind shear was balanced was identified, while the rest of the QLCS was cold pool dominant (Figure 13). Thus, the warning forecaster's primary focus would be on this balanced region of the QLCS.

For the second ingredient, the 0-3 km line normal wind shear was analyzed. For this, it is important to identify the motion of the QLCS at the location previously identified as cold pool-wind shear balanced. In this case, the QLCS was moving to the northeast, or out of about 230°. The 0-3 km shear vectors at and slightly downstream of the QLCS were about 40 knots out of the due south (180°). Using trigonometry, the line normal 0-3 km wind shear was found to be around 25 knots (Figure 14). Thus, the second ingredient was not quite satisfied at this time.

For the third ingredient, a rear-inflow notch was identified in the reflectivity field (Figure 15). A small appendage was also present on the leading edge of the QLCS accompanying the rear-inflow notch. This appendage was also co-located with what appeared to be a localized enhancement in the outbound velocity along the leading edge of the QLCS. However, no bowing segments were identified at this time. No strong velocity couplets occurred in the general time period analyzed here, and no tornadoes were reported. However, if a mesovortex was to have occurred, it very likely would have been at or near the location of the appendage in reflectivity. Thus, the Three-Ingredient Method here still served to draw attention to this location.

d. First Tornadic Period of the QLCS and the Three-Ingredient Method

Moving forward in time around 90 minutes, or to around 04z on 20 February 2017 (10 pm CST 19 February), the QLCS was entering the western side of the San Antonio metro (Bexar County). At this time, it was a fragmented QLCS lacking organization and lacking a tight reflectivity gradient along the leading edge. However, the QLCS was entering into a more favorable environment, as analyzed from the 04z RAP model run. Namely, low level shear had increased, with 0-1 km shear up to 20 knots and 0-3 km shear up to about 40 knots.

The Three-Ingredient Method will be applied to the QLCS at 430z on 20 February 2017 (1030 pm CST on 19 February 2017) as the QLCS was located across central Bexar County and impacting the city of San Antonio, Texas.

For the first ingredient, a large portion of the QLCS was cold pool-wind shear balanced, encompassing the entirety of the QLCS across Bexar County. This region is encapsulated by the white rectangle in Figure 16.

At this time, a recent surge in the QLCS across the southern half of Bexar County had changed the motion of the QLCS line from around 230° to around 210°. This created a more favorable wind shear orientation, with 0-3 km shear vectors of 40 knots out of around 175° yielding 0-3 km line normal shear closer to 35 knots and satisfying the second ingredient (Figure 17). It is important to note here that the 0-3 km shear did not increase, but the change in QLCS motion created a more favorable orientation, thereby increasing the line normal shear.

For the third ingredient, a well-defined rear-inflow notch was present associated with the bowing segment of the QLCS through central Bexar County (Figure 18). An outflow surge was also apparent in the velocity image, with enhanced inbound velocities present associated with the southern half of the bowing segment. This bowing segment likely helped to create a localized enhanced updraft at the location of the UDCZ, increasing low-level rotation. As mentioned earlier, this surge also acted to change the motion of the QLCS from 230° to 210°, increasing the line-normal 0-3 km wind shear. Lastly, a cross-section was taken through the bowing segment (using GR2 Analyst) along a radial from KEWX radar, thereby creating essentially a range height indicator (RHI) radar image. An analysis of this cross-section revealed what appeared to be a descending RIJ (Figure 19). Thus, it is clear that the third ingredient was very much satisfied at this point in time.

A total of four (4) tornadoes occurred between 436z and 500z in Bexar County and neighboring Comal County from this QLCS. One of these four tornadoes was rated EF-2, with a 5 mile path through north-central San Antonio and the city of Alamo Heights. An example of some of the damage caused by this tornado can be found in Figure 20 as well as a 4-panel radar image from this same tornado (Figure 21).

e. Second Tornadic Period of the QLCS and the Three-Ingredient Method

Moving ahead to 620z (1220 am CST 20 February), the QLCS of interest was east of Austin, Texas. At this point, all three ingredients were once again satisfied, with the biggest change from the previously analyzed time period being a marked increase in the line-normal 0-3 km wind shear, with values up to about 45 knots (Figure 22). Two additional EF-2 tornadoes occurred between 625z and 633z.

Conclusions and Best Practices

Once the warning forecaster (with the help of a mesoanalyst and backup radar personnel) has identified the location where all three ingredients are satisfied, they have also identified the specific region of the QLCS that is most favorable for mesovortexgenesis and thus tornadogenesis. Applying the QLCS motion and analyzing the shear vectors along and downstream of the QLCS can help determine the greatest

QLCS tornado threat area over the next 0 to 30-45 minutes (see Figure 23). If a tornado warning has not already been issued, it is suggested that a tornado warning should be strongly considered once all three ingredients have been met. Convey this information to core partners, such as local media and emergency manager, via NWS Chat and any other appropriate platforms.

Given the rapidly changing situation of a QLCS event and the effort required to employ the Three-Ingredient Method, it is strongly recommended that a team of at least three people be used during warning operations. It is important to have a devoted mesoanalyst keeping a close watch on the 0-3 km bulk shear vectors along and downstream of the QLCS, as well as a backup radar operator periodically determining the cold pool-wind shear balance regimes and searching for any indications of bowing segments or outflow surges. For determining the 0-3 km line normal shear, the RAP 0-3 km bulk shear wind barbs can be overlaid on the radar data, or the SPC Mesoanalysis Page can be employed, with 0-3 km shear found under the multi-parameter fields section. All three members of this warning team need to continually keep each other updated on the status of the three ingredients, and information can even be projected onto a situational awareness display for more effective viewing.

It is important to note that the Three-Ingredient Method is not perfect. QLCS mesovortices and tornadoes can and do still occur when all three ingredients are not satisfied. Similarly, all three ingredients may be satisfied but the QLCS still may not produce mesovortices and/or tornadoes. The Three-Ingredient Method tends to be the most useful during wintertime and springtime QLCS events when wind shear is stronger. Summertime QLCSs in which bow echoes may occur in the presence of very large instability but weak wind shear may occasionally produce tornadoes. In these instances, the 30 knots of 0-3 km line normal wind shear is very unlikely to be met. Strong rotational signatures in velocity should always be paid close attention to for possible tornadogenesis regardless of whether or not the three ingredients are met.

Ultimately, the Three-Ingredient Method should be employed as a tool to better anticipate QLCS mesovortexgenesis and tornadogenesis. Utilizing the Three-Ingredient Method has the potential to greatly enhance warning forecaster situational awareness during QLCS events and has promising implications for improving POD and lead times for QLCS tornadoes.

References

Atkins, N. T., and M. S. Laurent, 2009: Bow Echo Mesovortices. Part I: Processes That Influence Their Damaging Potential. *Mon. Wea. Rev.*, **137**, 14971513

Atkins, N. T. and M. St. Laurent, 2009: Bow Echo Mesovortices. Part II: Their Genesis. *Mon. Wea. Rev.*, **137**, 1514–1532.

Brotzge, J., S. E. Nelson, R. L. Thompson, and B. T. Smith, 2013: Tornado probability of detection and lead time as a function of convective mode and environmental parameters. *Wea. Forecasting*, **28**, 1261- 1276.

Funk, T.W., K.E. Darmofal, J.D. Kirkpatrick, V. L. Dewald, R. W. Przybylinski, G. K. Schmocker, and Y.-J Lin, 1999: Storm reflectivity and mesocyclone evolution associated with the 15 April 1994 squall line over Kentucky and southern Indiana. *Wea. Forecasting*, **14**, 976993.

Houze, R. A., Jr.: Mesoscale convective systems, *Rev. Geophys*., **42**, RG4003.

Newman, J. F, and P. L. Heinselman, 2012: Evolution of a Quasi-Linear Convective System Sampled by Phased Array Radar. *Mon. Wea. Rev.*, **140:11**, 3467-3486.

Schaumann, J. S., and R. W. Przybylinski, 2012: Operational Application of 0-3 km Bulk Shear Vectors in Assessing QLCS Mesovortex and Tornado Potential. Preprints, *26th Conf. on Severe Local Storms*, Nashville, TN, Amer. Meteor. Soc., 9.10.

Schenkman, A., M. Xue, and A. Shapiro, 2012: Tornadogenesis in a simulated mesovortex within a mesoscale convective system. *J. Atmos. Sci.*, **69**, 3372–3390.

Smith, B.T., R.L. Thompson, J.S. Grams, C. Broyles and H.E. Brooks, 2012: Convective modes for significant severe thunderstorms in the contiguous United States. Part I: Storm classification and climatology. *Wea. Forecasting*, **27**, 1114-1135.

Tessendorf, S. A. and R. J. Trapp, 2000: On the climatological distribution of tornadoes within quasi-linear convective systems. Preprints, 20th Conf. on Severe Local Storms, Orlando, FL, Amer. Meteor. Soc., 134-137.

Trapp, R. J., S. A. Tessendor, E. S. Godfrey, and H. E. Brooks, 2005: Tornadoes from squall lines and bow echoes. Part I: Climatological distribution. *Wea. Forecasting*, **20**, 23–34.

Weisman, M. L., and R. J. Trapp, 2003: Low level vortices within squall line and Bow Echoes: Part I. Overview and dependence on environmental shear. *Monthly Weather Review*, **131**, 2804-2823.

Weisman, M. L., and R. J. Trapp, 2003: Low level vortices within squall line and Bow Echoes: Part II. Their genesis and implications. *Monthly Weather Review*, **131**, 2804-2823.

Wheatley, D. M., and R. J. Trapp, 2008: The Effect of Mesoscale Heterogeneity on the Genesis and Structure of Mesovortices within Quasi-Linear Convective Systems. *Mon. Wea. Rev.*, **136**, 4220–4241.

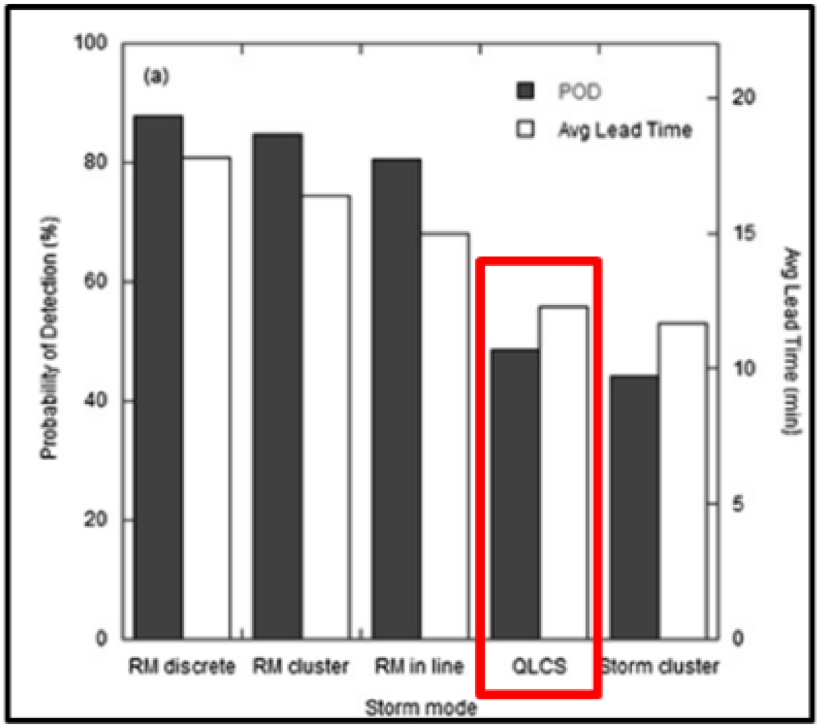

Figure 1: Tornado POD and average lead time for various storm morphologies from all nationwide tornado events from 2003 to 2004 from Brotzge et al. (2013).

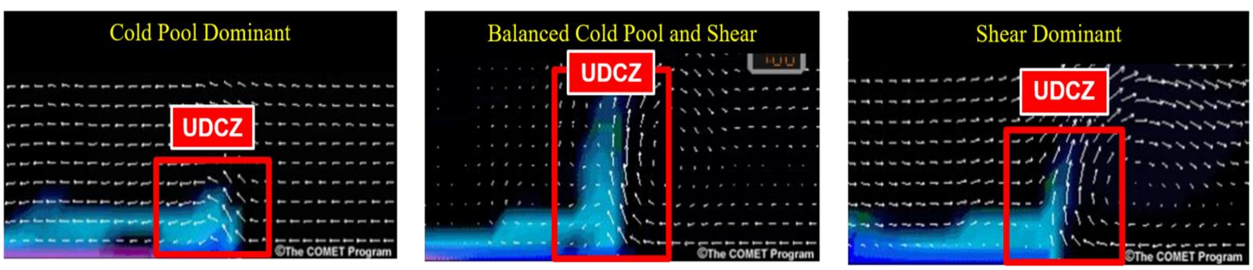

Figure 2: Depth of the Updraft/Downdraft Convergence Zone (UDCZ) for cold pool dominant QLCSs (left), balanced cold pool and wind shear QLCSs (middle) and shear dominant QLCS (right). This is the basis of the first ingredient of the method.

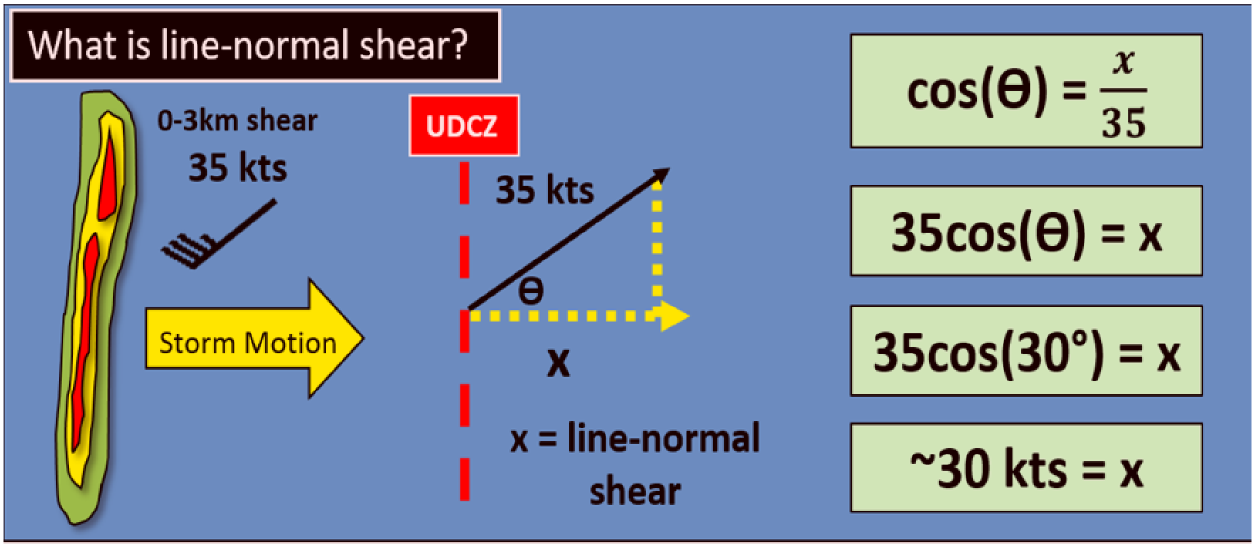

Figure 3: Image depicting the calculation of line-normal wind shear for the second ingredient of the Three-Ingredient Method. Calculation requires the magnitude of the wind shear vector as well as the computation of the angle between the wind shear direction and the motion of the QLCS.

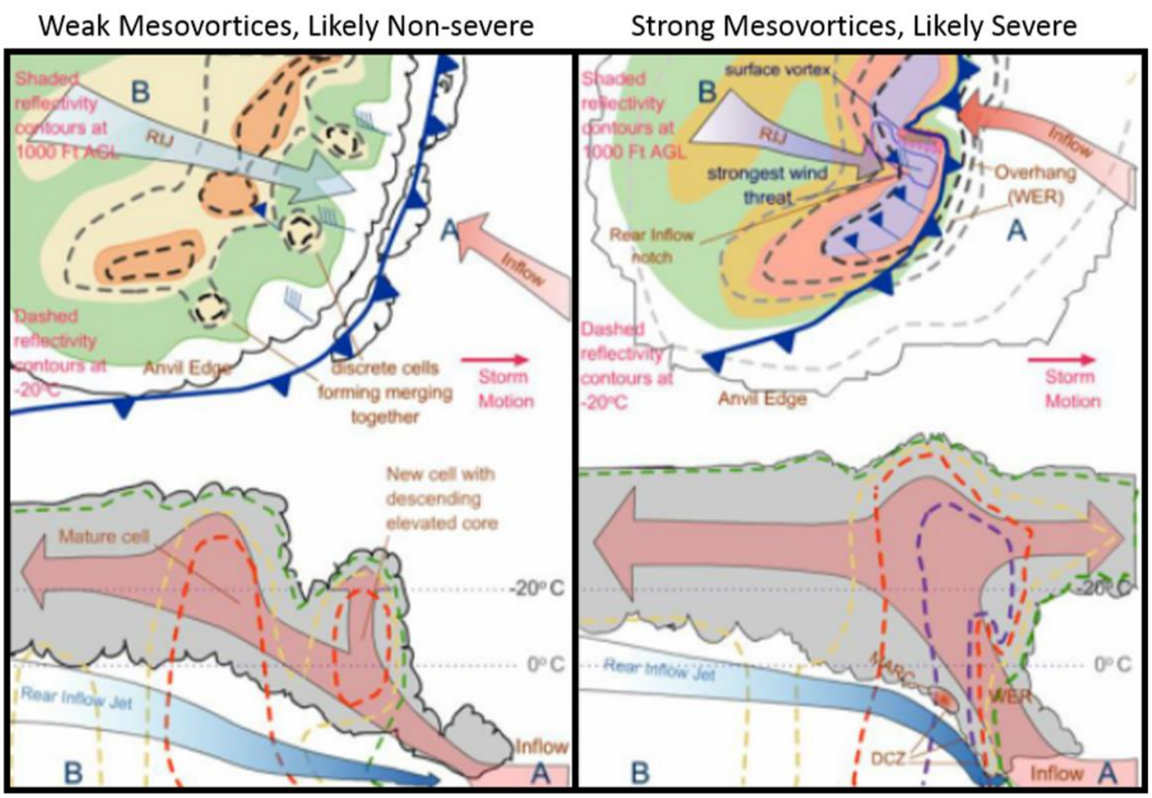

Figure 4: Example of an MCS in which the cold pool is dominant (non-severe, left) and an MCS in which the cold pool and environmental wind shear is well-balanced (severe, right). Figure from Jim Ladue and Ron Przybylinkski from IC Severe 3 Storm interrogation best practices for 3D QLCS structures 2010 NOAA WDTB.

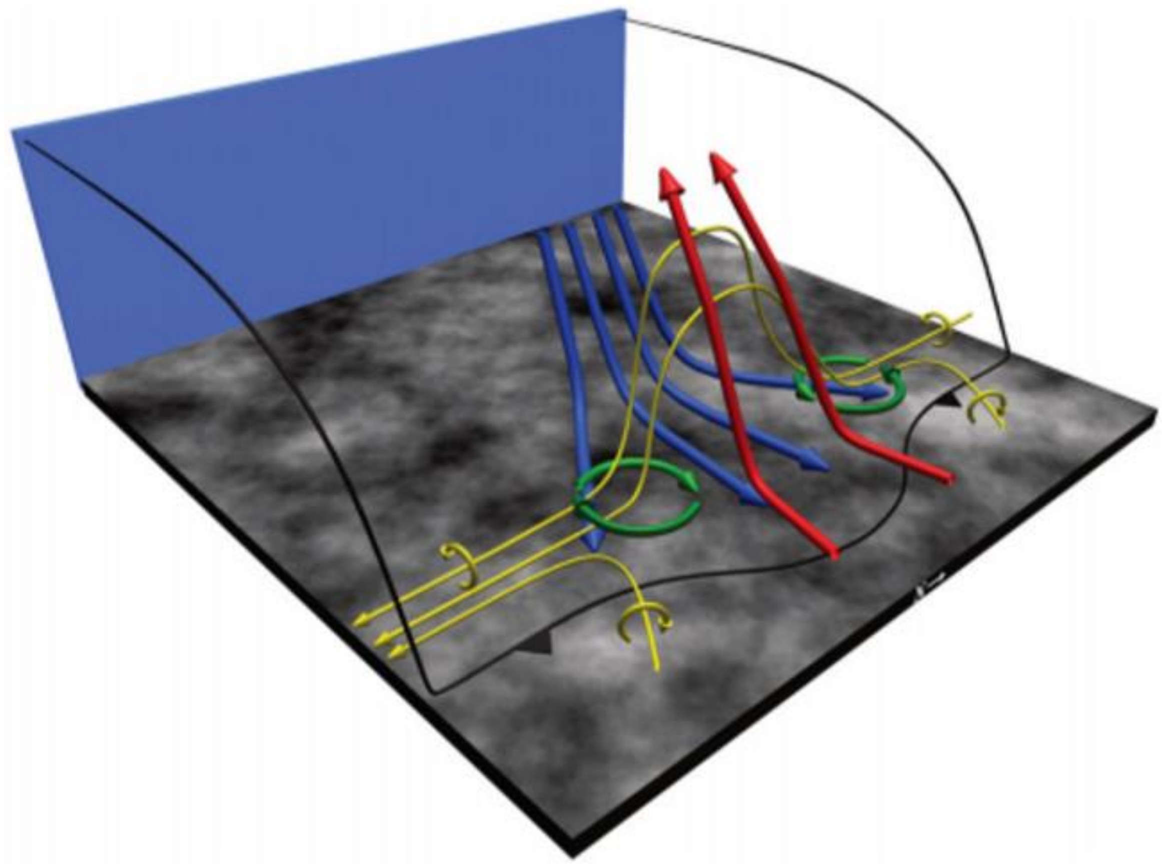

Figure 5: Schematic diagram of cyclonic-anticyclonic mesovortex genesis. Vortex lines (gold), inflow and updraft (red), and downdraft (blue) are all depicted. The thick green arrow represents the mesovortex. The gust front position is shown in black. From Atkins and St. Laurent (2009 Part II).

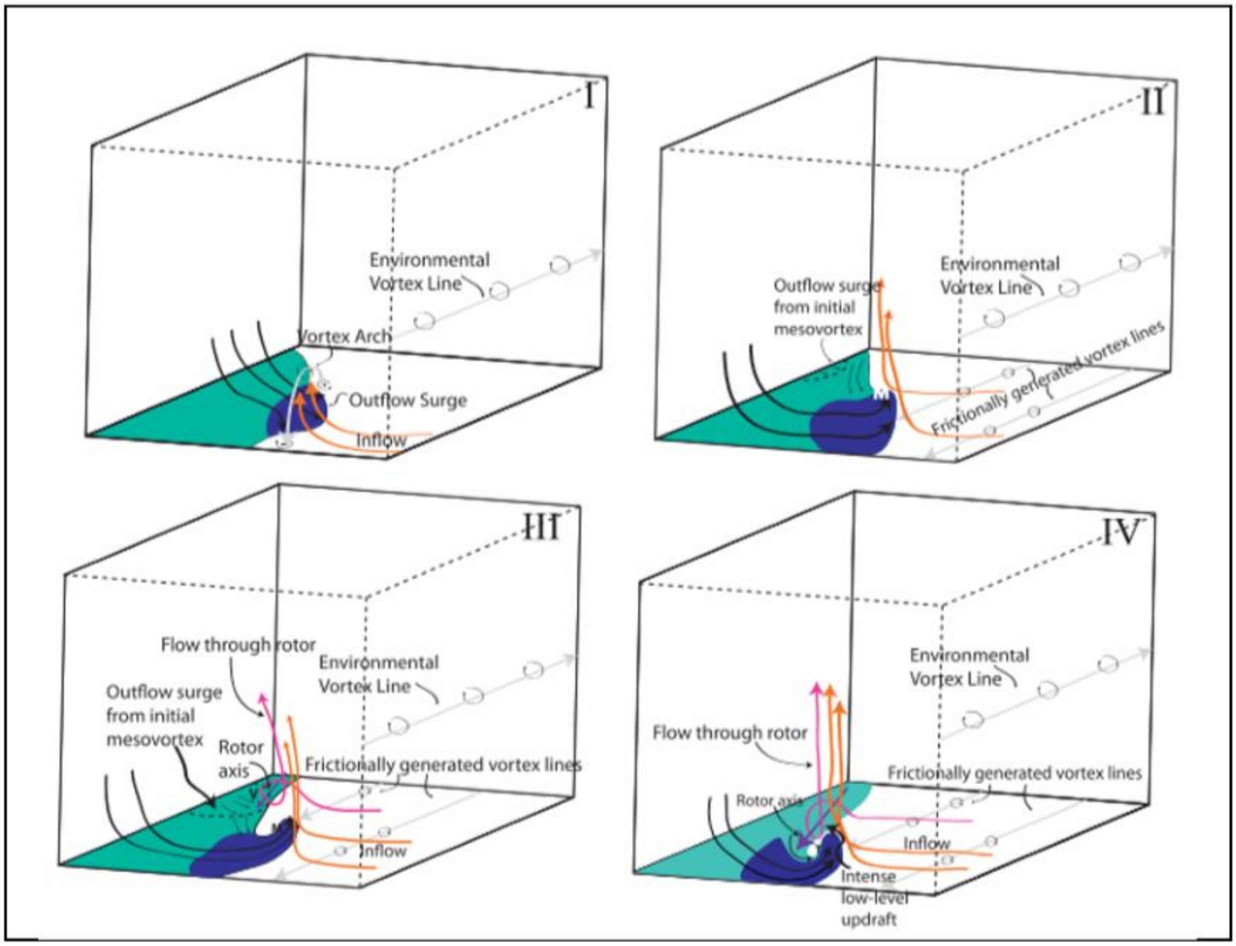

Figure 6: Schematic of four-stage process leading up to tornado-like vortex (TLV) genesis: vertical vorticity couplet development (I), development of the dominant cyclonic Minco mesovortex and the associated development of frictionally generated horizontal vorticity (II), development of the rotor (III), and TLV genesis (IV). Cyan shading represents the cold pool. Dark blue shading represents the cold air within the cold pool bulge. Black arrows represent the surface flow trajectories. Orange arrows represent trajectories that enter the main updraft. Purple arrow in (III) in (IV) marks the horizontal rotor axis. Magenta arrows represent parcel trajectories that enter the rotor. Light gray vectors are idealized vortex lines. The "M" represents the location of the Minco mesovortex. Dotted curves in (II) and (III) mark the location of the enhanced westerly momentum associated with the dissipation of the initial mesovortex. The "V" behind the outflow surge from the initial mesovortex in (III) marks the location of the small area of vertical vorticity moving through the rotor. The "T" marks the location of the TLV. (From Schenkman et al. 2012)

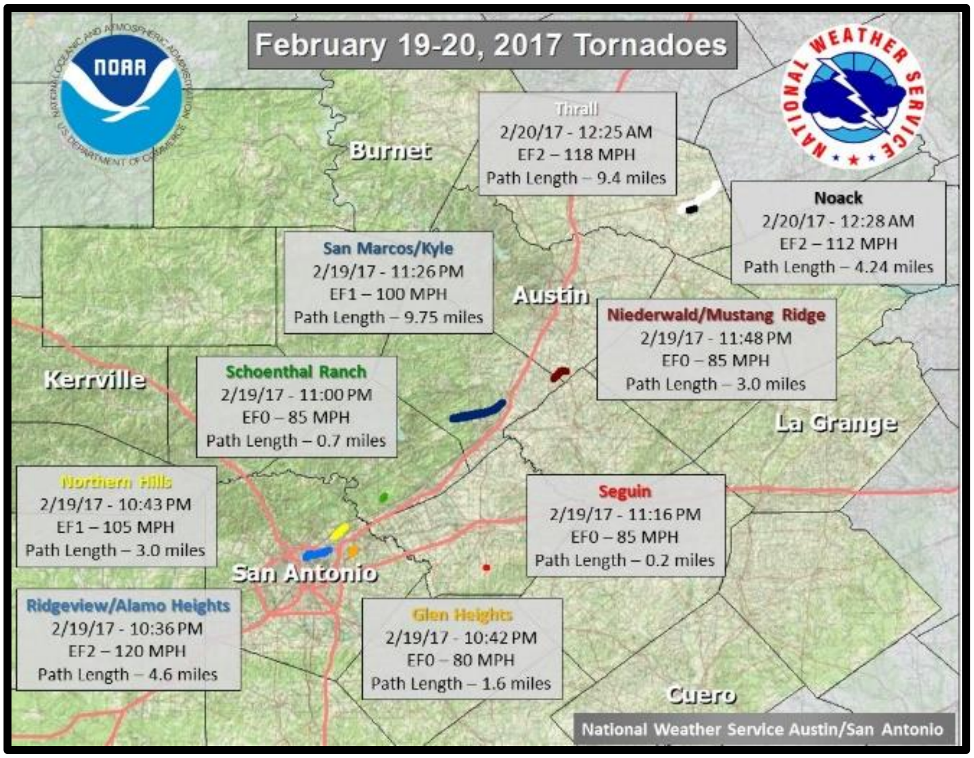

Figure 7: All nine (9) confirmed tornadoes from the 19-20 February 2017 tornadic QLCS event across the Austin/San Antonio CWA. Information includes start time of each tornado, EF rating, max wind speeds and total path length.

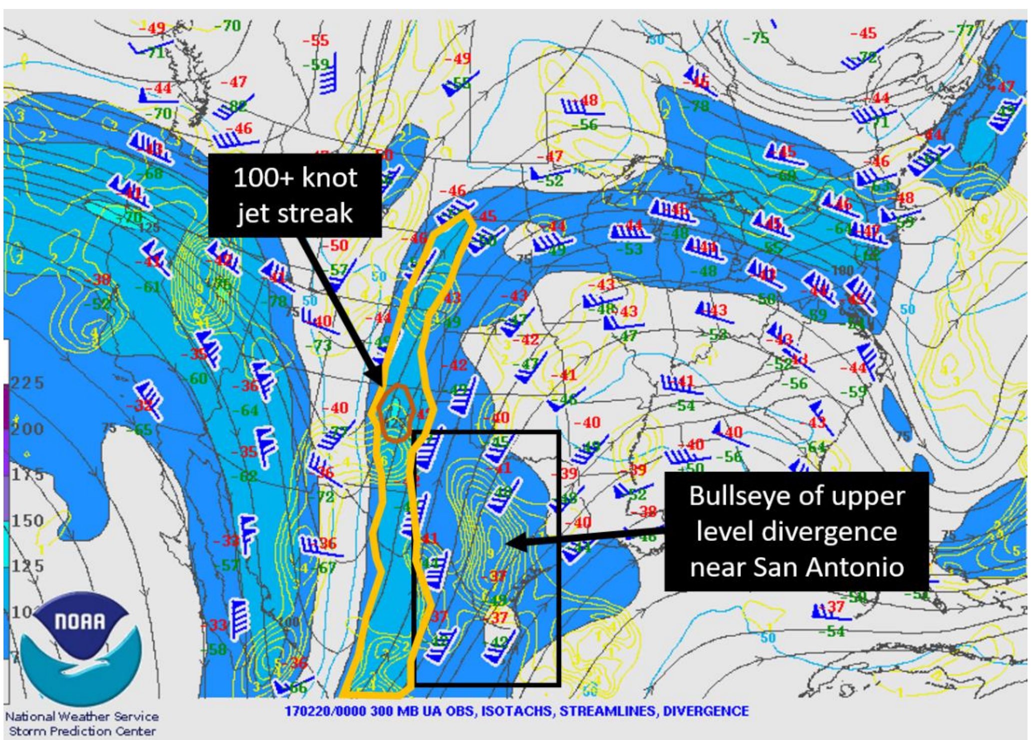

Figure 8: 300 hPa analysis from 00z 20 February 2017.

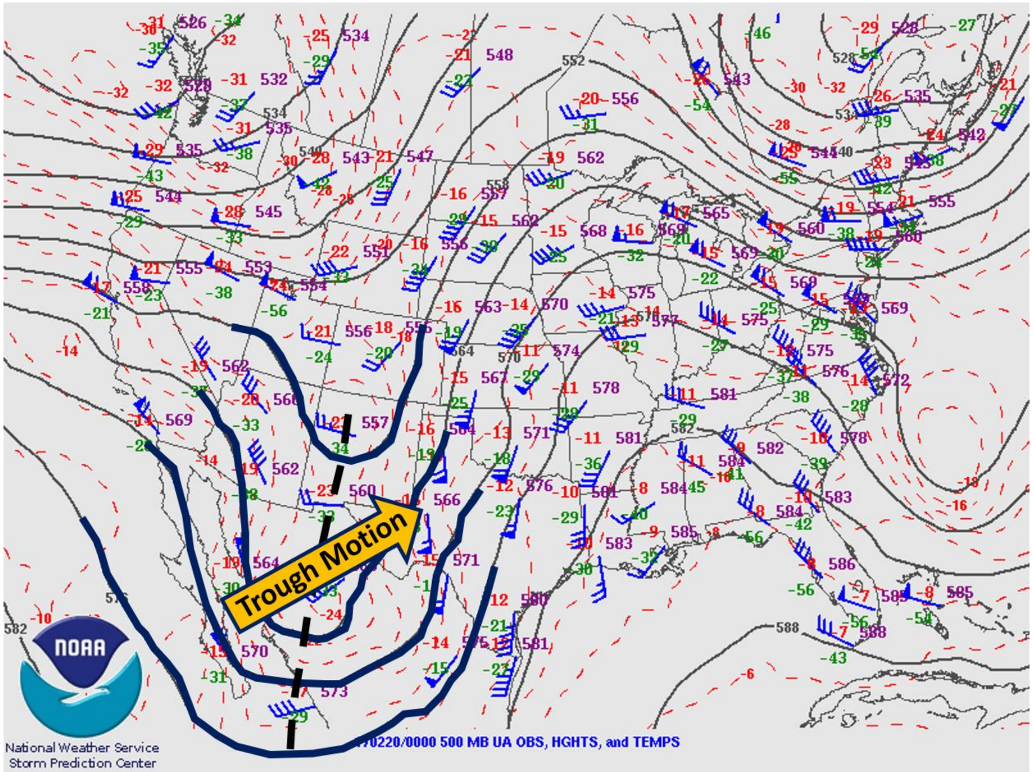

Figure 9: 500 hPa analysis from 00z 20 February 2017

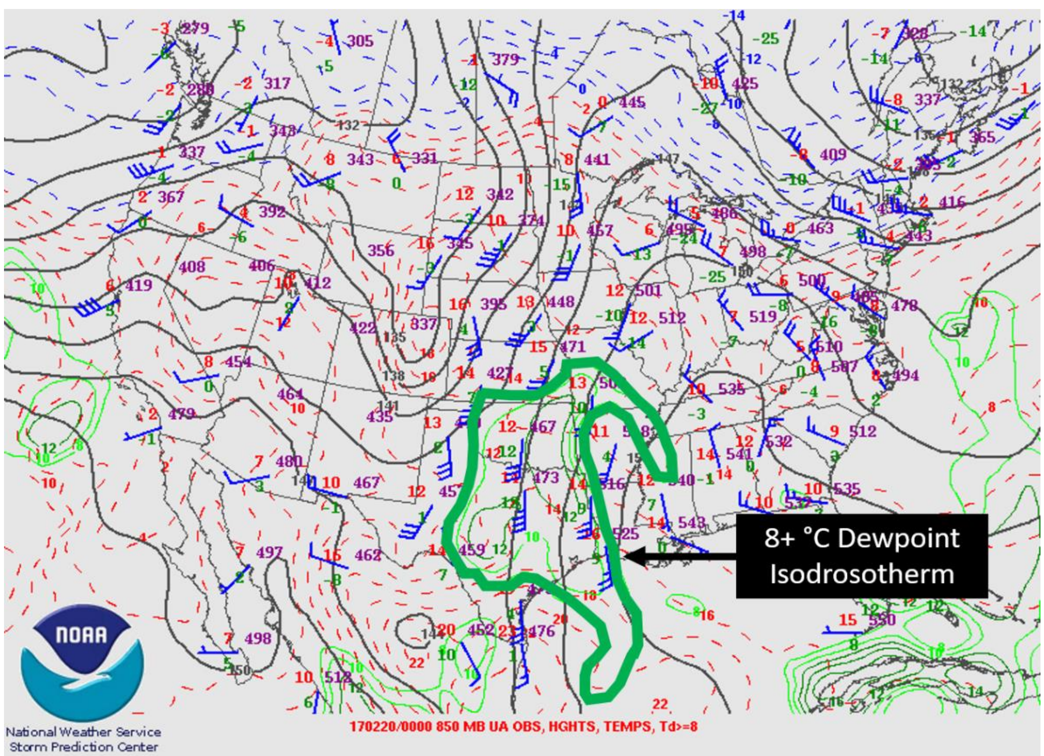

Figure 10: 850 hPa analysis from 00z 20 February 2017

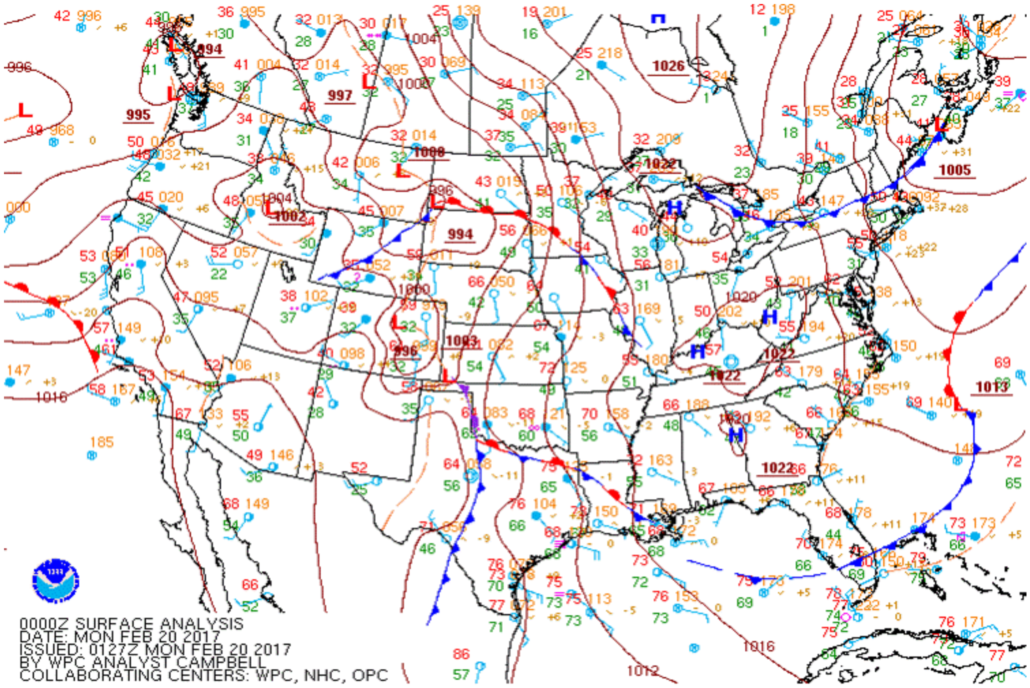

Figure 11: WPC Surface Analysis from 00z 20 February 2017

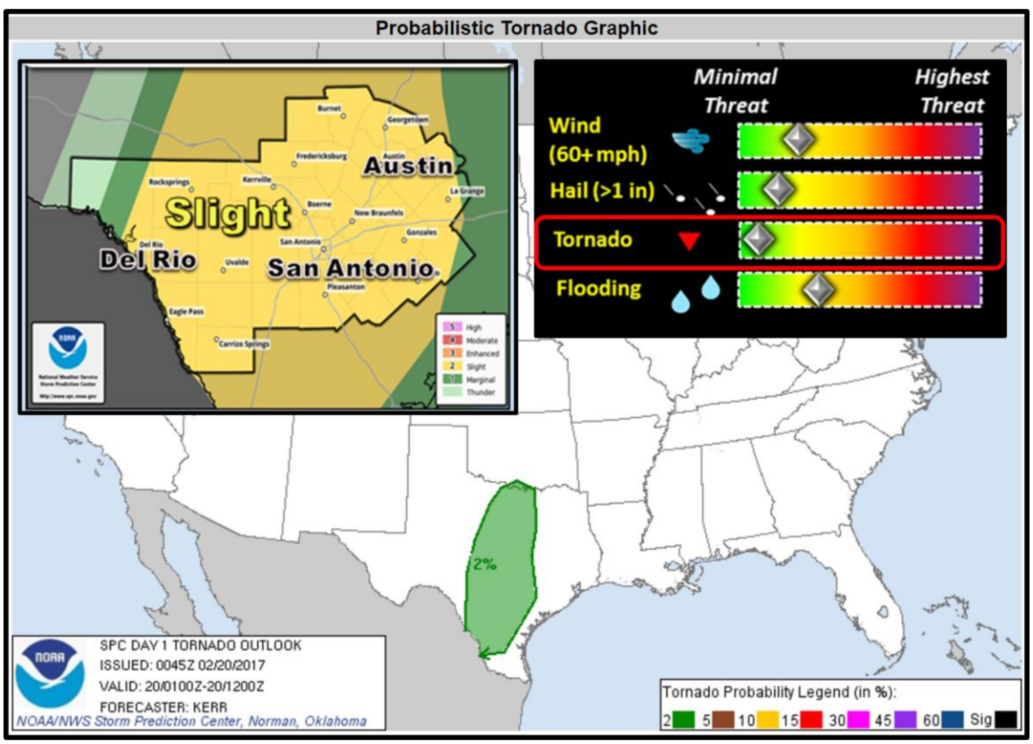

Figure 12: 01z 20 February 2017 Day 1 SPC Convective Outlook (top left), 01z 20 February 2017 Day 1 SPC Probabilistic Tornado Graphic (bottom) and graphic created from WFO Austin/San Antonio showing the threat level for various severe hazards (top right).

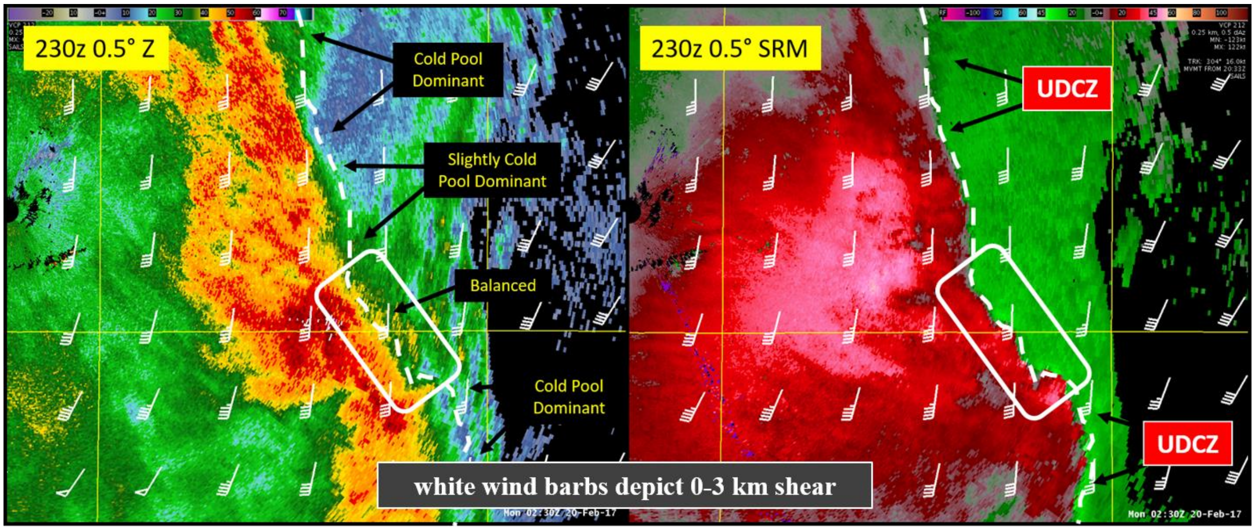

Figure 13: 0.5° Reflectivity (left) and 0.5° SRM (right) from KDFX radar at 230z on 20 February 2017. In the right image, the UDCZ is identified with the white dashed line. The UDCZ is then overlaid on the reflectivity image on the left, and the cold pool-wind shear regimes are identified. The location encapsulated by the white rectangle denotes the region of the QLCS where the QLCS is cold pool-wind shear balanced, and thus where the first ingredient is satisfied.

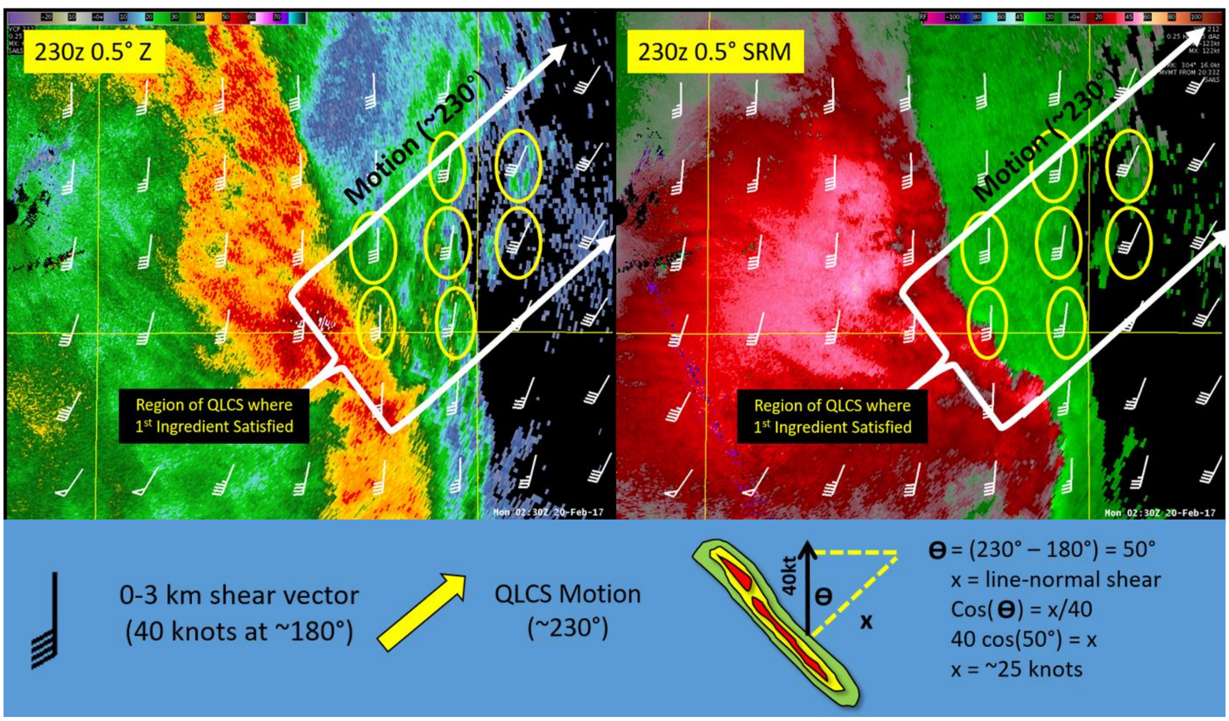

Figure 14: Same as Fig. 13, but with the 0-3 km shear vectors along and downstream of the cold pool-wind shear balanced regime of the QLCS encircled and the motion of the QLCS displayed. Beneath this is the calculation of the line-normal 0-3 km wind shear for the analysis of the second ingredient.

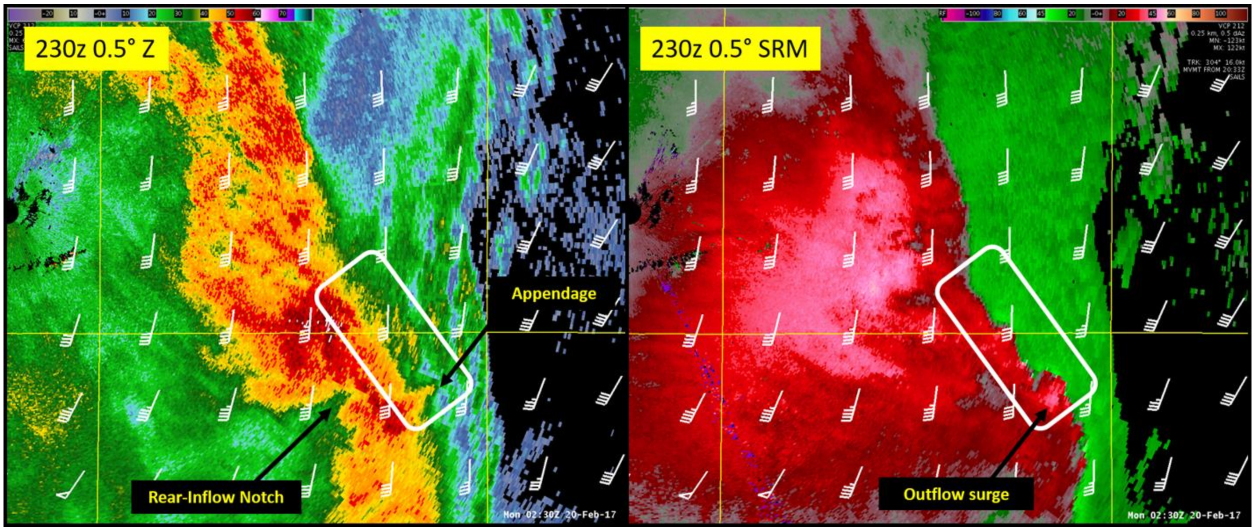

Figure 15: Same as Fig 13., but with the radar images annotated with the location of a rear-inflow notch and associated appendage in reflectivity (left) and an outflow surge in velocity (right). The white rectangle depicts the location of the QLCS where the first ingredient is satisfied.

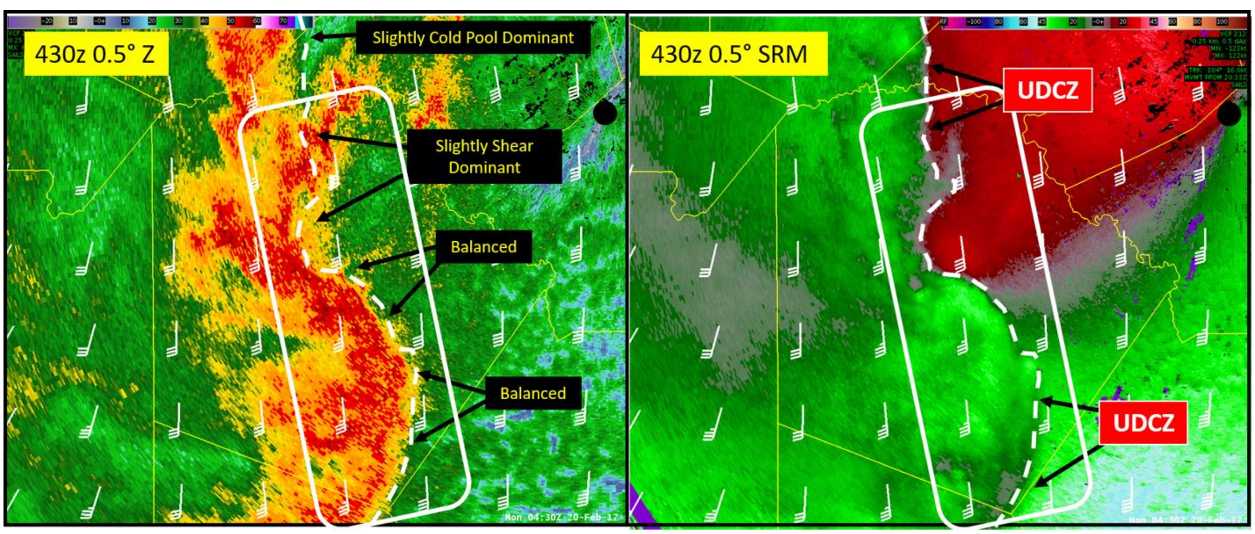

Figure 16: 0.5° Reflectivity (left) and 0.5° SRM (right) from KEWX radar at 430z on 20 February 2017. In the right image, the UDCZ is identified with the white dashed line. The UDCZ is then overlaid on the reflectivity image on the left, and the cold pool-wind shear regimes are identified. The location encapsulated by the white rectangle denotes the region of the QLCS where the QLCS is cold pool-wind shear balanced, and thus where the first ingredient is satisfied.

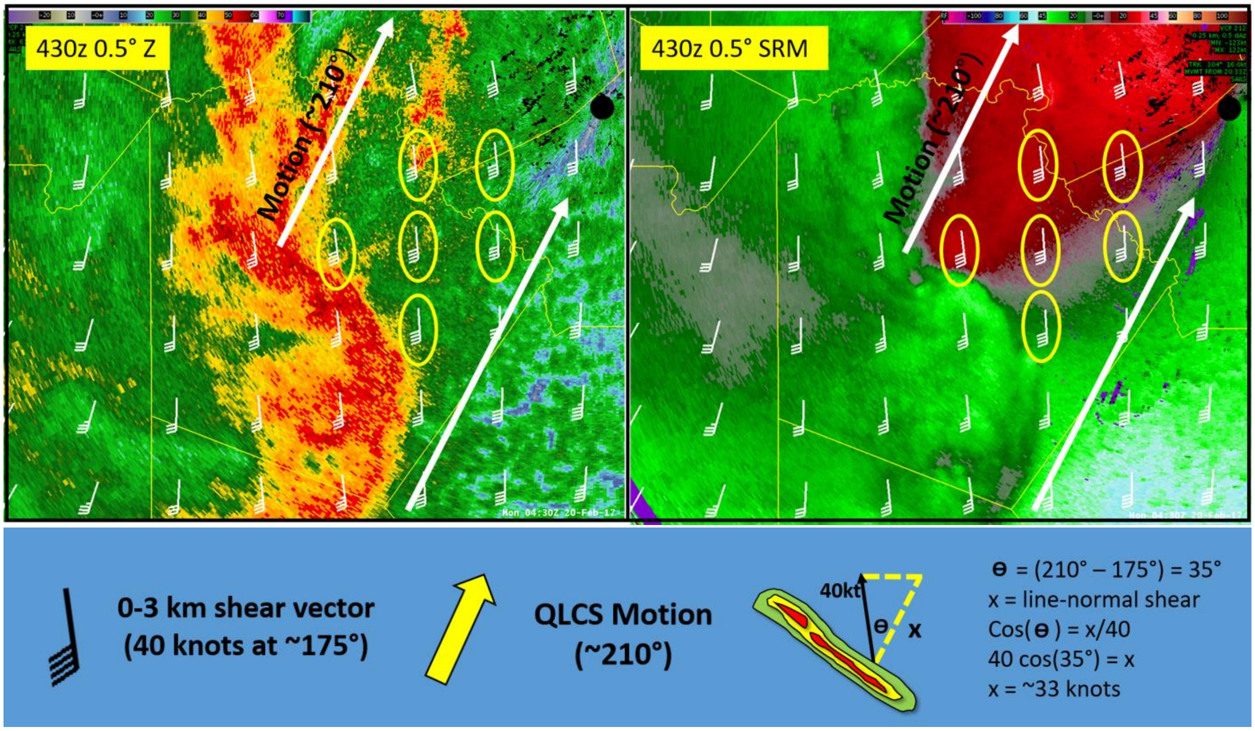

Figure 17: Same as Fig. 16., but with the 0-3 km shear vectors along and downstream of the cold pool-wind shear balanced regime of the QLCS encircled and the motion of the QLCS displayed. Beneath this is the calculation of the line-normal 0-3 km wind shear for the analysis of the second ingredient.

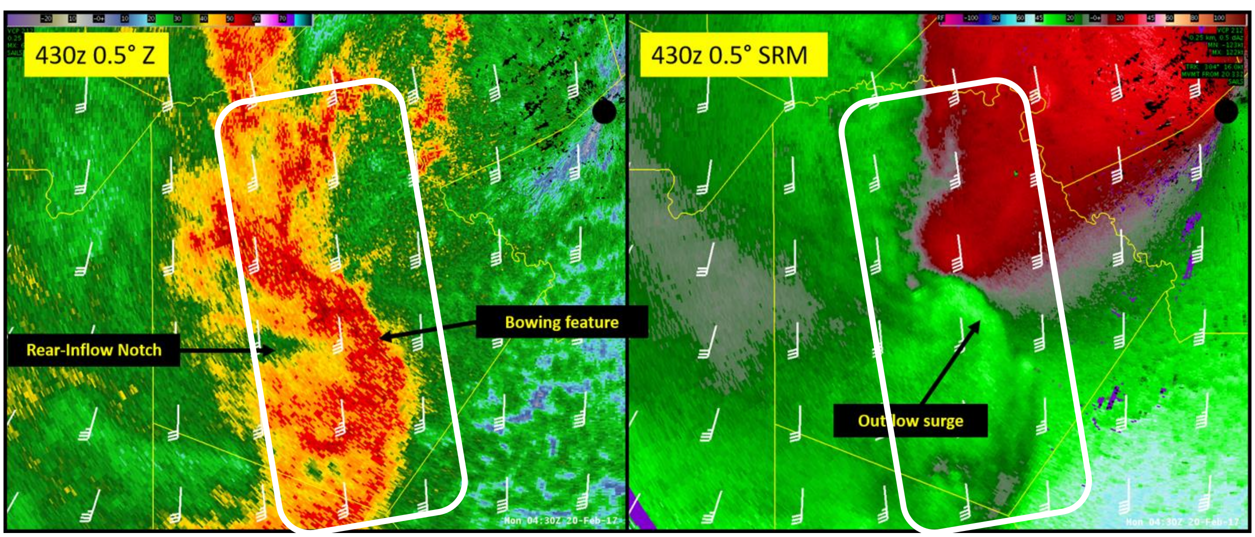

Figure 18: Same as Fig 16., with the radar images annotated with the location of a rear-inflow notch and associated bowing feature in reflectivity (left) and an outflow surge in velocity (right). The white rectangle depicts the location of the QLCS where the first ingredient is satisfied.

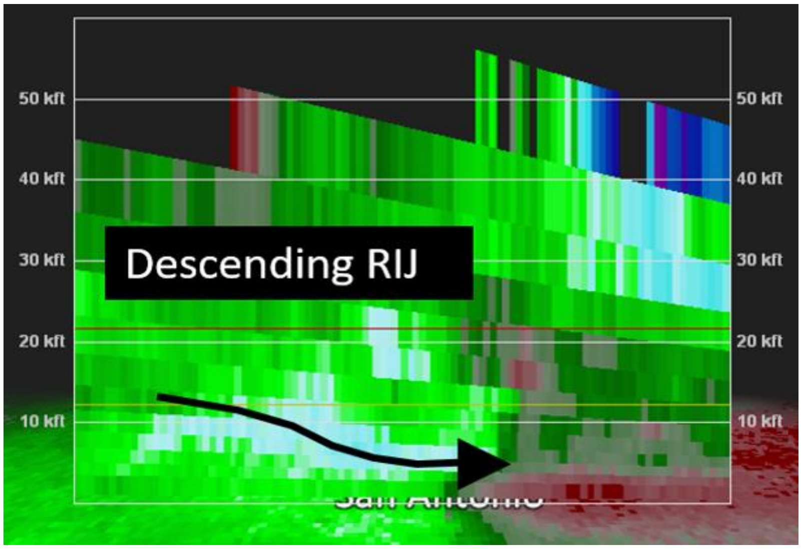

Figure 19: Cross-section in velocity taken using GR2Analyst along a radial from KEWX radar through the bowing segment of the QLCS in central Bexar County. A descending RIJ appears to be present.

Figure 20: Aerial photograph taken on the afternoon of 21 February 2017 of damage from the EF-2 tornado that impacted portions of north-central San Antonio and the city of Alamo Heights on the evening of 19 February 2017. Photograph courtesy of Texas Civil Air Patrol.

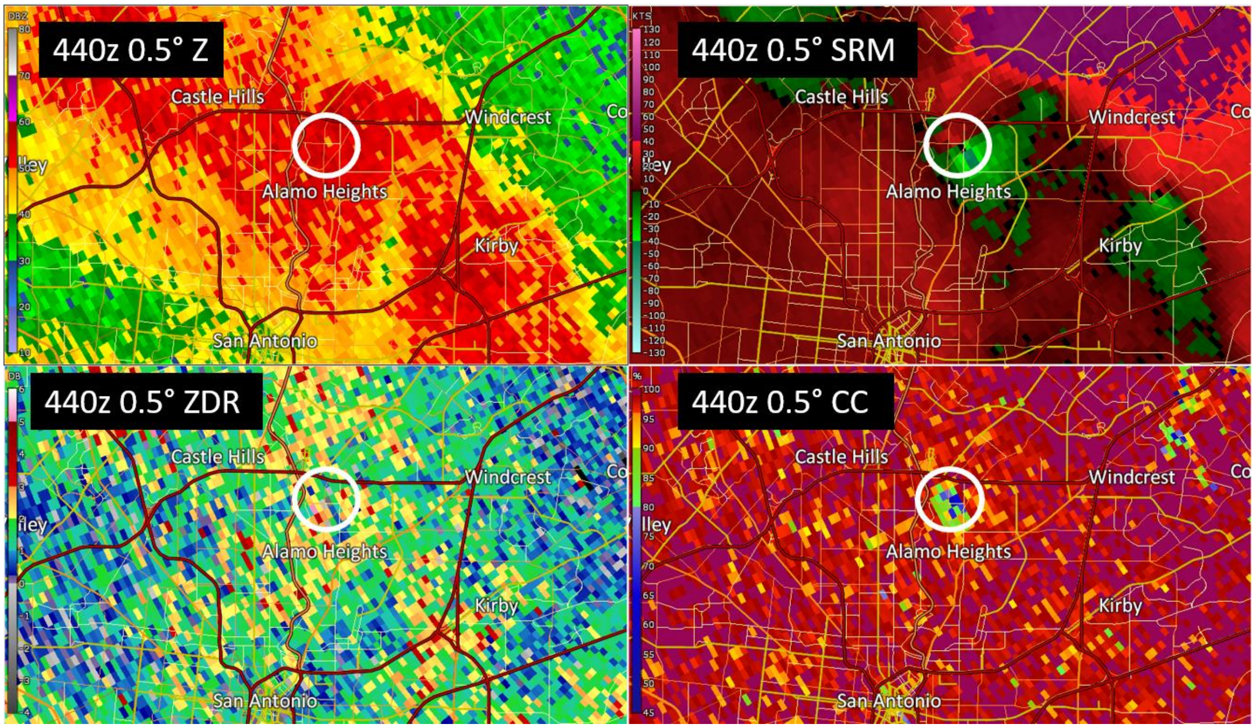

Figure 21: 4-panel radar image of 0.5° Reflectivity (top left), 0.5° SRM (top right), 0.5° Differential Reflectivity (bottom left) and 0.5° Correlation Coefficient (bottom right) at 440z 20 February 2017 from KEWX radar showing the EF-2 tornado that impacted north-central San Antonio and the city of Alamo Heights (encircled region). Note the presence of a tornado debris signature associated with the tornado.

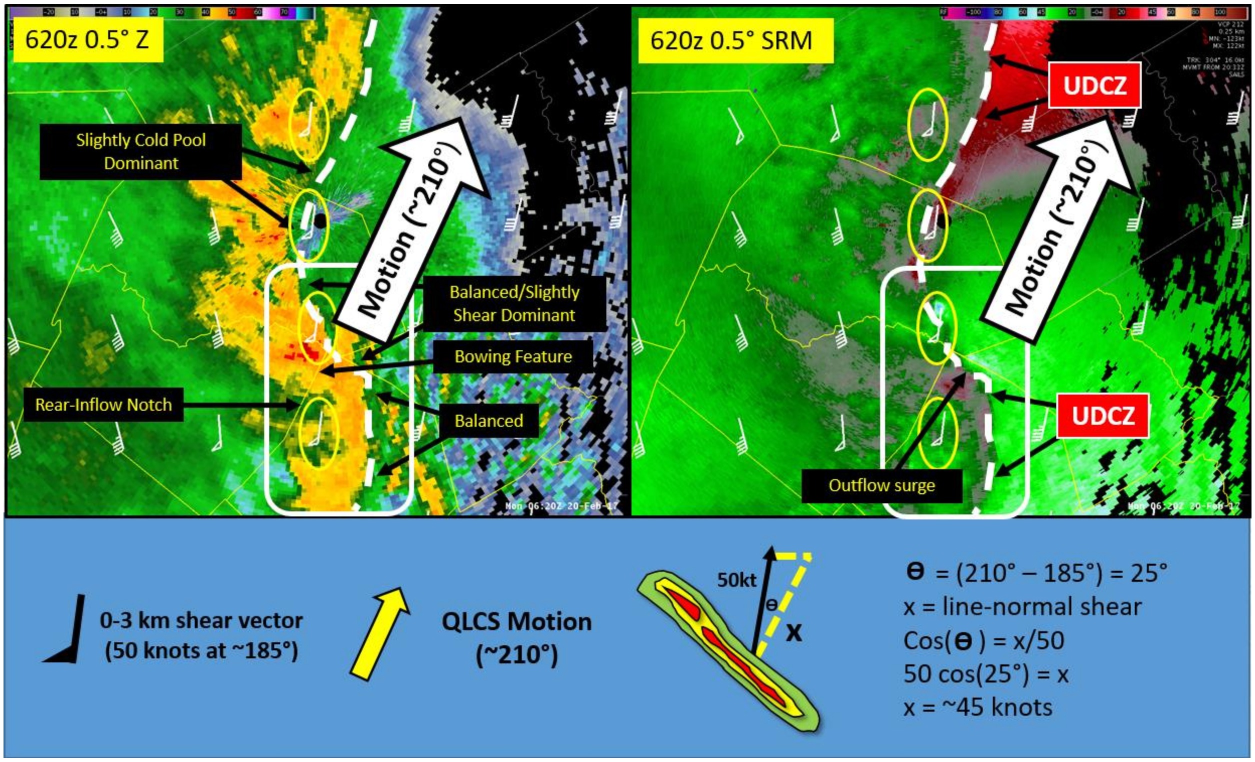

Figure 22: 0.5° Reflectivity (left) and 0.5° SRM (right) from KEWX radar at 620z on 20 February 2017. In the right image, the UDCZ is identified with the white dashed line. The UDCZ is then overlaid on the reflectivity image on the left, and the cold pool-wind shear regimes are identified. The location encapsulated by the white rectangle denotes the region of the QLCS where the QLCS is cold pool-wind shear balanced or slightly shear dominant, and thus where the first ingredient is satisfied. Next, 0-3 km shear vectors along and downstream of the cold pool-wind shear balanced regime of the QLCS are encircled and the motion of the QLCS displayed. Beneath this is the calculation of the line-normal 0-3 km wind shear for the analysis of the second ingredient. Lastly, a rear-inflow notch and small bowing feature is analyzed in reflectivity in the left image.

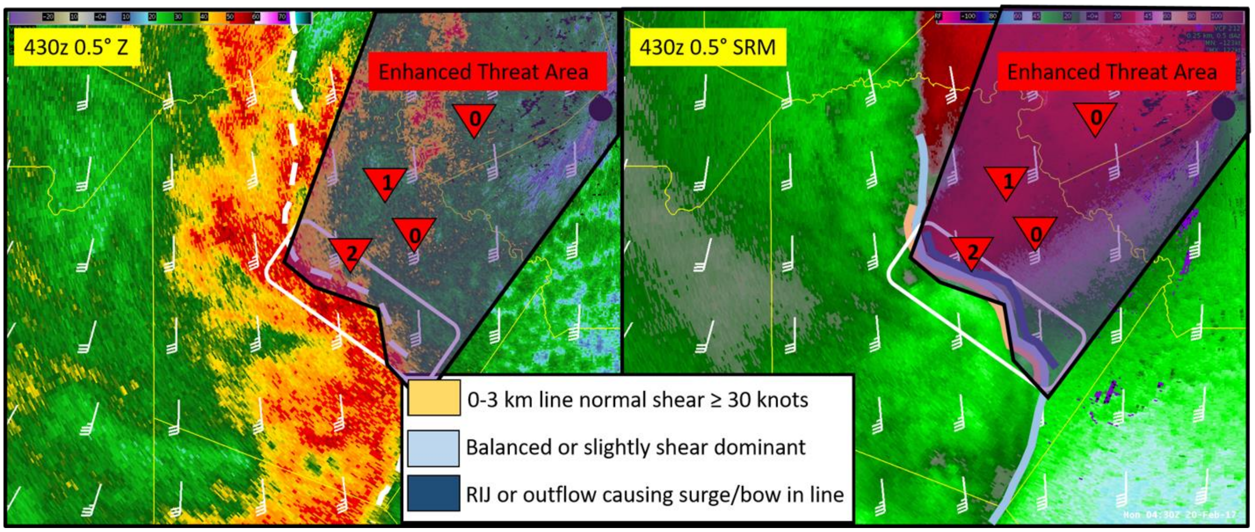

Figure 23: 0.5° Reflectivity (left) and 0.5° SRM (right) from KEWX radar at 430z on 20 February 2017. This figure shows the creation of the Enhanced Threat Area for QLCS mesovortexgenesis and tornadogenesis in the time from of 0 to 30-45 minutes. The specific location of the QLCS where each individual ingredient is satisfied is shown in the SRM image on the right. The location where all three ingredients are satisfied is denoted by the white rectangle. Then, by using the QLCS motion and seeing that the 0-3 km shear vectors downstream of the QLCS will allow for the second ingredient to remain satisfied, an enhanced threat area for QLCS mesovortexgenesis and tornadogenesis can be created. The red triangles denote the location of the four tornadoes that occurred between 436z and 500z on 20 February 2017 and their respective EF ratings.